inorganics

Article

Gadolinium(III)-DOTA Complex Functionalized with BODIPY as a Potential Bimodal Contrast Agent for MRI and Optical Imaging

Matthias Ceulemans, Koen Nuyts, Wim M. De Borggraeve and Tatjana N. Parac-Vogt *

Department of Chemistry, KU Leuven, Celestijnenlaan 200F, Leuven 3001, Belgium;
E-Mails: Matthias.Ceulemans@chem.kuleuven.be (M.C.); Koen.Nuyts@chem.kuleuven.be (K.N.);
Wim.DeBorggraeve@chem.kuleuven.be (W.M.D.B.)

* Author to whom correspondence should be addressed; E-Mail: Tatjana.Vogt@chem.kuleuven.be;
Tel.: +32-16-327-612.

Abstract: The synthesis and characterization of a novel gadolinium(III) DOTA complex functionalized with a boron-dipyrromethene derivative (BODIPY) is described. The assembly of the complex relies on azide diazotransfer chemistry in a copper tube flow reactor. The azide thus formed is coupled directly with an alkyne via click chemistry, resulting into a paramagnetic and luminescent gadolinium(III) complex. Luminescent data and relaxometric properties of the complex have been evaluated, suggesting the potential applicability of the complexes as a bimodal contrast agent for magnetic resonance and optical imaging. The complex displays a bright emission at 523 nm with an absorption maximum of 507 nm and high quantum yields of up to 83% in water. The proton relaxivity of the complex measured at 310 K and at frequencies of 20 and 60 MHz had the values of 3.9 and 3.6 $s^{-1} \cdot mM^{-1}$, respectively.

Keywords: Gadolinium(III); BODIPY; click chemistry; MRI; contrast agent

1. Introduction

Magnetic resonance imaging (MRI) is a diagnostic tool that has experienced large growth over the past years. Consequently, the search for highly-efficient, responsive, and tissue-specific markers has

followed the same trend. Most of the clinically-used contrast agents are based on gadolinium(III) chelates [1–6]. Gadolinium(III), with its symmetric $^8S_{7/2}$ ground state and large magnetic moment (7.94 μ_B), is a superior ion to efficiently increase relaxation rates of water molecules [1]. Due to the toxicity of free gadolinium(III) (LD$_{50}$ = 0.2 mmol·kg^{-1} in mice), and the fact that relative high concentrations of contrast agents are needed for MRI scan (up to 0.3 mmol per kg body weight) [7,8], strong chelating agents are used to ensure kinetic and thermostatic stability of the gadolinium(III) complex. The most widespread contrast agents used in modern molecular imaging techniques are the acyclic diethylenetriaminepentaacetic acid (Gd(III)-DTPA, Magnevist®, Bayer Healthcare, Berlin, Germany) and the cyclic 1,4,7,10-tetraazacyclododecane-1,4,7,10-tetraacetic acid (Gd(III)-DOTA, Dotarem®, Guerbet, Hongkong, China) [2]. The eight-fold coordination ensures high stability (log$K$ = 25.3 and 20.1 for DOTA and DOTA-propylamide respectively), and allows the binding of one water molecule directly to the metal center [9–12].

MRI excels in its special resolution and depth penetration, but it suffers from a low sensitivity. Combining it with a complimentary imaging technique would allow for obtaining a better diagnostic tool, as it was recently demonstrated by a successful combination of MRI and PET probes [13–15]. The combined contrast agent gives both insight into the morphology (MRI) and information about biomedical processes (PET) of the human body. Another promising imaging modality complementary to MRI is optical imaging, which has a very good sensitivity, but lacks the spatial resolution and depth penetration. The latter drawback can be circumvented by choosing the absorption and emission wavelength close to the biological window [16]. Different optical probes have already been coupled to DTPA or DOTA, such as luminescent polymers in lipophilic aggregates [17], luminescent metal complexes [18–27], dendrimers [28], and organic dyes such as quinolone [29], rhodamine [30,31], fluoresceine [32], and naphalimide [33,34].

A promising class of organic dyes are 4,4-Difluoro-4-bora-3a,4a-diaza-s-indacene (abbreviated as BODIPY) and its derivatives. This class of small organic molecules generally has very high extinction coefficients, fairly sharp fluorescence peaks, and high quantum yields. The BODIPY core is pretty stable in physiological conditions and relatively insensitive to the environment. Their emission wavelength is tunable by increasing the resonance within the BODIPY core [35]. The BODIPY dyes have been used in a variety of applications such as biological labels and probes [36–38], fluorescent probes [39], laser dyes [40,41], light emitting diodes [42], solar cells [43,44], and potential sensitizers in photodynamic therapy [45,46]. Although BODIPYs are versatile compounds with good optical properties, their use in developing bimodal contrast agents remain scarce [47–52]. ^{18}F labeled BODIPY derivatives have been recently suggested as bifunctional reporters for hybrid optical/positron emission tomography imaging [53,54]. An example of DOTA ligand functionalized with BODIPY compound was reported in 2010 by Bernhard *et al.* [47] with the idea to generate a bimodal imaging agent for optical and nuclear imaging (PET/CT) by introducing In(III), Ga(III) and Cu(II) into the DOTA moiety. In 2012 the same group expanded their compound to a DOTAGA derivative (GA = glutaric acid) which gave more stable complexes with the transition metals [48,51,52]. Considering the versatility and favorable optical properties of BODIPY organic dyes, there are surprisingly very few examples of its use as an optical probe in the development of bimodal contrast agents. The main disadvantage of BODIPY dyes is their hydrophobicity, which limits their solubility and therefore hinders their straightforward application as a probe for medical imaging. Although overcoming the

solubility issue poses a challenge, it is also beneficial as it was demonstrated that hydrophilic dyes can improve cell permeability [50].

We have recently shown that BODIPY dyes can be functionalized in a copper tube flow reactor via chemistry that converts primary amines into azides using the catalyst generated *in situ* from the metallic copper [55]. In this paper we further expand this strategy for performing azide-alkyne cycloaddition in order to create a Gd-DOTA-BODIPY derivative. We report on the synthesis and characterization of this novel compound and evaluate its potential as a bimodal contrast agent for MRI and optical imaging.

2. Results and Discussion

2.1. Synthesis of Gd-DOTA-BODIPY Derivative

The main concept used in order to create a Gd-DOTA-BODIPY derivative is based on using click chemistry to couple a BODIPY dye to a DOTA moiety, resulting in a bimodal agent with both optical and paramagnetic entities (Figure 1). The novel BODIPY derivative developed in this work is 5,5-difluoro-1,3,7,9-tetramethyl-10-(2-(4-((2-gadolinium(III)-(4,7,10-tris(carboxylatomethyl)-1,4,7,10-tetraazacyclododecan-1-yl)acetamido)methyl)-1H-1,2,3-triazol-1-yl)ethyl)-5H-dipyrrolo[1,2-c:2′,1′-f][1,3,2]diazaborinin-4-ium-5-uide, presented in Figure 1. The synthesis of the BODIPY core starts with the protection of β-analine with phtalic acid in solvent free conditions. Subsequently reaction with thionyl chloride converts the acid group into an acid chloride, which can react further with two equivalent of 2,4-dimethylpyrrole to form a dipyrromethene derivative. Complexation of this product with borontrifluoride dietherate and a base forms BODIPY-$(CH_2)_2$-phtalimide. This product can easily be transformed into BODIPY-$(CH_2)_2$-amine by using hydrazine in ethanol, which was clearly demonstrated by the disappearance of the aromatic peaks at 7.77 and 7.88 ppm, and appearance of a new peak at 1.61 ppm in the ^{1}H NMR spectrum (Scheme 1). The final BODIPY product contains an amine function which can be transformed in a copper tube into an azide via a diazotranfer reagent (ISA·H_2SO_4) giving BODIPY-$(CH_2)_2$-azide shown in Figure 2a [56,57].
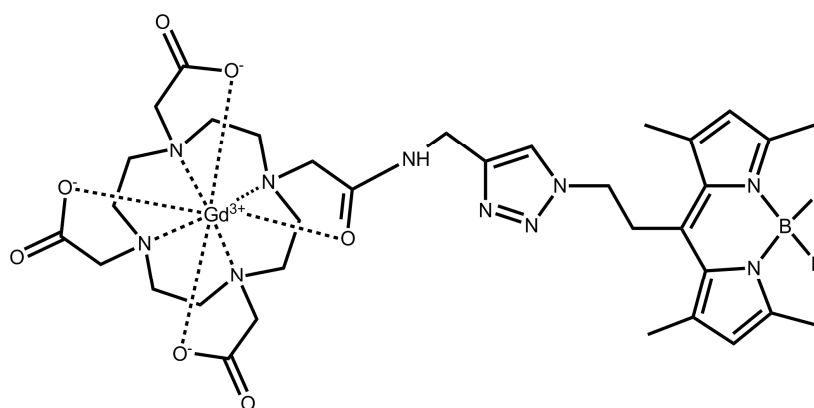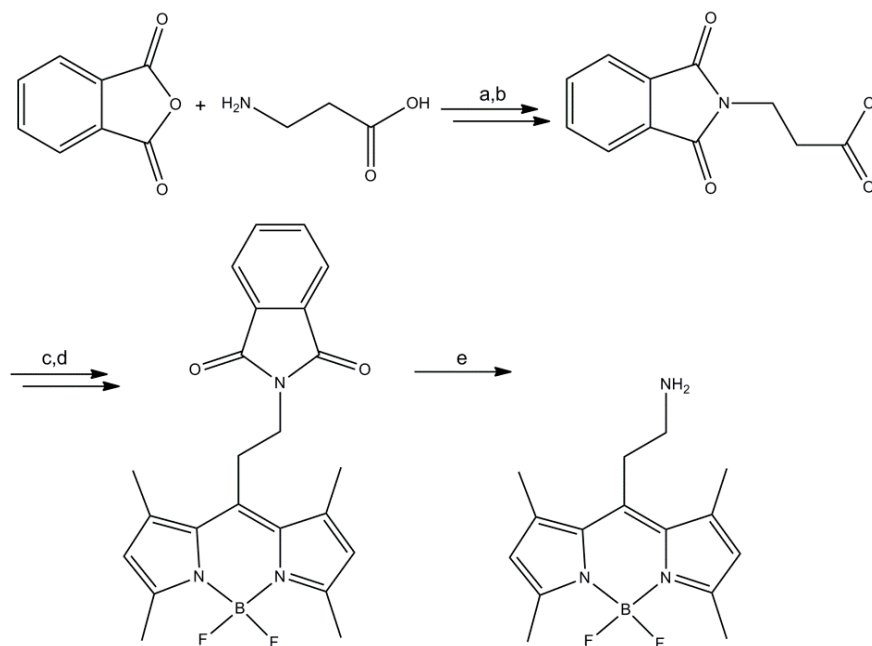

Figure 1. The Gd-DOTA-BODIPY derivative.

Scheme 1. Synthetic procedure for BODIPY-$(CH_2)_2$-amine: (**a**) 160 °C, 6 h; (**b**) $SOCl_2$, reflux, 3 h; (**c**) 2 equivalents 2,4-dimethylpyrrole, DCM, 0 °C reflux, 4 h; (**d**) 10 eq. DIPEA, 11 eq. $BF_3 \cdot Et_2O$, DCM, 0 °C R.T., overnight; and (**e**) $N_2H_4 \cdot H_2O$, EtOH, reflux, 3 h.

The propargylated Ln(III)-DOTA complex (Ln = La, Gd) that was used for coupling to BODIPY dye is shown in Figure 2b [58,59]. The coupling was performed by using a flow chemistry approach, which can mitigate some safety related issues regarding working with azides [60]. Organic azides can be synthesized from primary amines via a diazotransfer reaction. The potential short shelf life and highly explosive nature of some diazotransfer reagents requires their careful consideration of the safety issues for their handling [61]. Some safety issues can be circumvented by introduction of imidazole-1-sulfonyl azide (ISA) or its hydrogen sulfate salt (ISA·H_2SO_4) [56,62]. The flow reaction was performed by mixing solutions of BODIPY-$(CH_2)_2$-amine and ISA·H_2SO_4, which is graphically represented in Scheme 2. Upon leaving the reactor, the reaction mixture was directly added to a solution of propargylated Ln(III)-DOTA (Ln = La or Gd), resulting in the final product Ln(III)-DOTA-BODIPY.
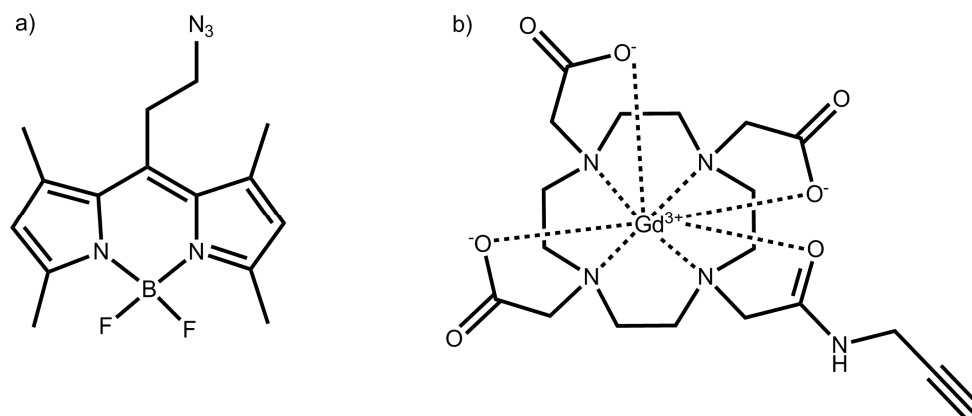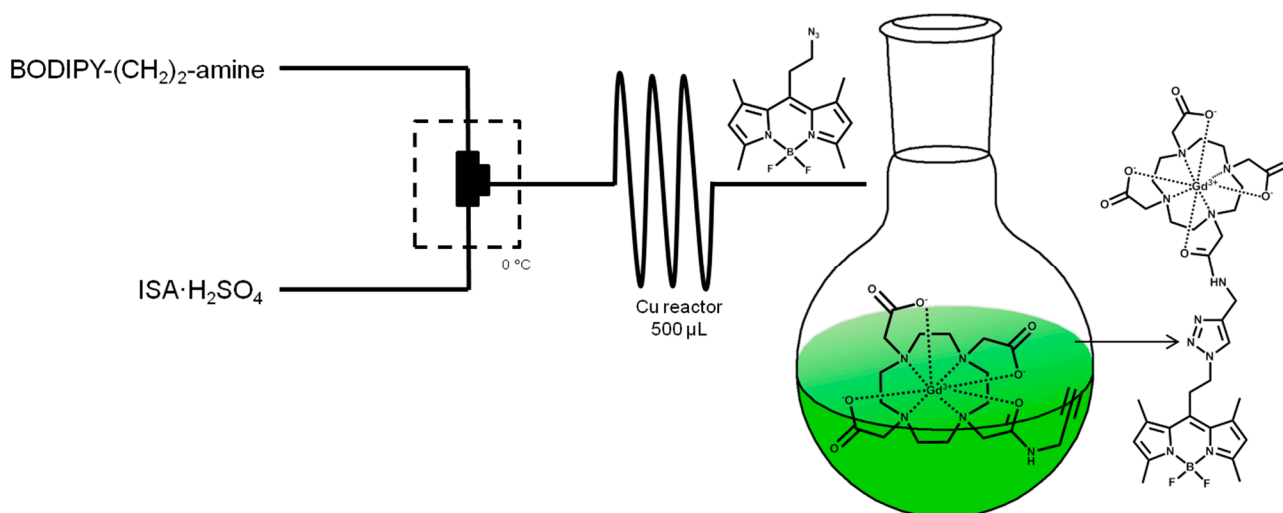

Figure 2. (**a**) Structure of BODIPY-$(CH_2)_2$-azide made in a copper tube reactor; (**b**) Structure of propargylated Gd(III)-DOTA complex used to couple to the azide.

Scheme 2. Schematic representation of the flow reactor.

The Ln-DOTA-BODIPY complexes have been isolated and purified (see Figure S13) and the diamagnetic lanthanum(III) complex La-DOTA-BODIPY has been characterized by ^{1}H NMR spectroscopy in solution (Figure 3). The ^{1}H NMR spectrum shows a distinct peak of the triazole proton at 7.55 ppm and two protons on the BODIPY core at 6.00 ppm, indicating a successful linkage of the DOTA moiety with the BODIPY derivative. The ^{1}H NMR spectrum also shows broad peaks in the region from 2.20–3.82 ppm which are typical for the protons in the DOTA ring [63].
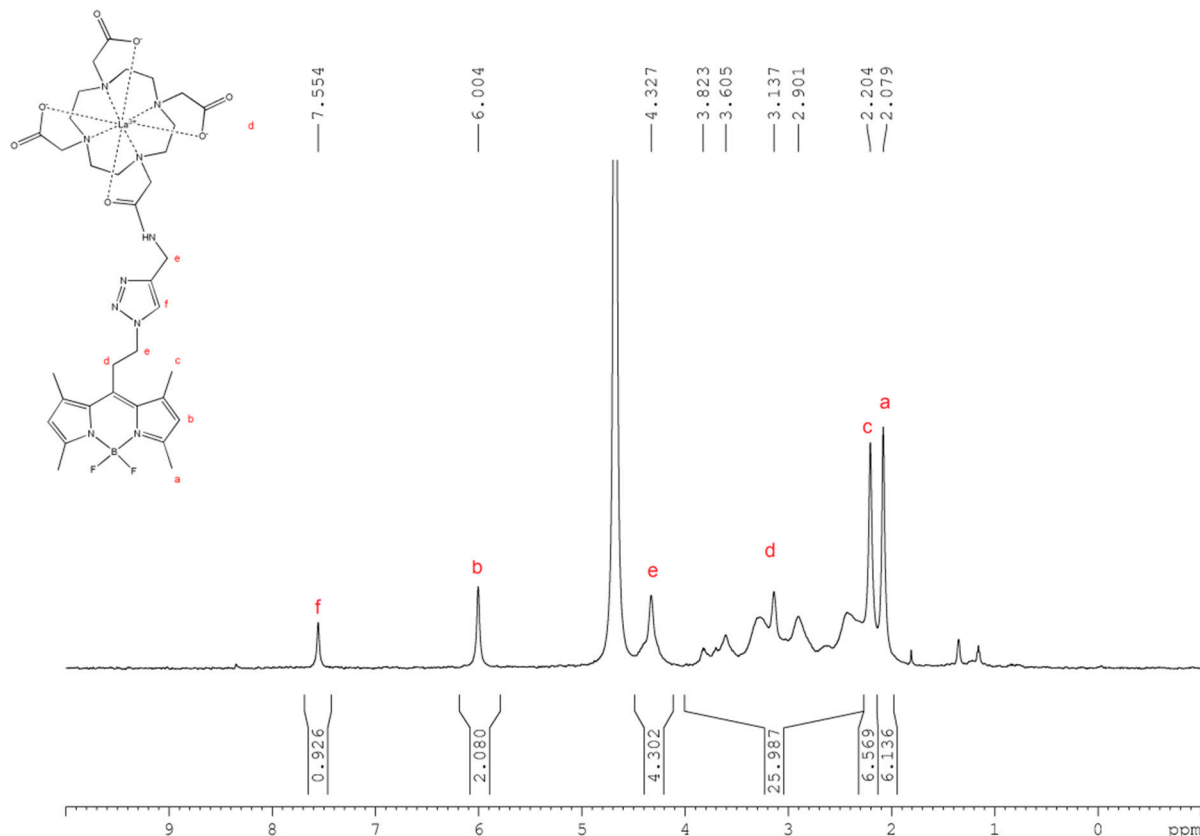

Figure 3. ^{1}H NMR spectrum of the final clicked La-DOTA-BODIPY derivative measured in deuterated water.

2.2. Photophysical Properties of the Gd-DOTA-BODIPY

The BODIPY derivatives are typically strongly red colored. Most BODIPY derivatives are apolar in nature and dissolve very well in apolar organic solvents, like chloroform or dichloromethane, and will emit a bright green fluorescence. Due to the coupling to hydrophilic Ln-DOTA complex the final Ln-DOTA-BODIPY adducts are water soluble and give bright green fluorescence in aqueous solution. Figure 4 shows a picture of an aqueous solution of the synthesized Gd-DOTA-BODIPY in the absence and in the presence of excitation light at 366 nm. The green fluorescence is clearly visible during excitation. Furthermore, the electronic spectra of Gd-DOTA-BODIPY are given in Figure 4 and depict the characteristic and rather narrow absorption and emission bands which are typical for BODIPY dyes. A main absorption band (blue dotted line) with a maximum λ_{abs}(max) at 503 nm is observed for Gd-DOTA-BODIPY in aqueous solution. These visible absorption bands can be assigned to the $S_0 \rightarrow S_1$ transition [64]. An additional, considerably weaker broad absorption band is observed in the UV-VIS region around 360 nm, and is attributed to the $S_0 \rightarrow S_2$ transition. It should be noted that the optical properties of the BODIPY dyes can be tuned by increasing conjugation through placing different substituents on the BODIPY core. Such substitutions increase the resonance of the whole structure and provide a red shift of the main emission band, which is favorable for biological applications. A tradeoff between tissue penetration and image resolution for *in vivo* imaging can be made in the optical imaging window (from 665 to 900 nm) [65]. In this region the extinction coefficients of the main sources of absorption such as hemoglobin, deoxyhemoglobin, and water, are at their minimum. However, it must be taken into account that placing additional substituents on the BODIPY usually renders the system more hydrophobic and decreases the solubility of the entire complex in water.

The emission maximum in water of Gd-DOTA-BODIPY (Figure 4) is observed at 523 nm and is in accordance with the previously reported BODIPY derivatives [66]. The excitation maximum (red dashed line) recorded at 560 nm shows a peak at 503 nm.
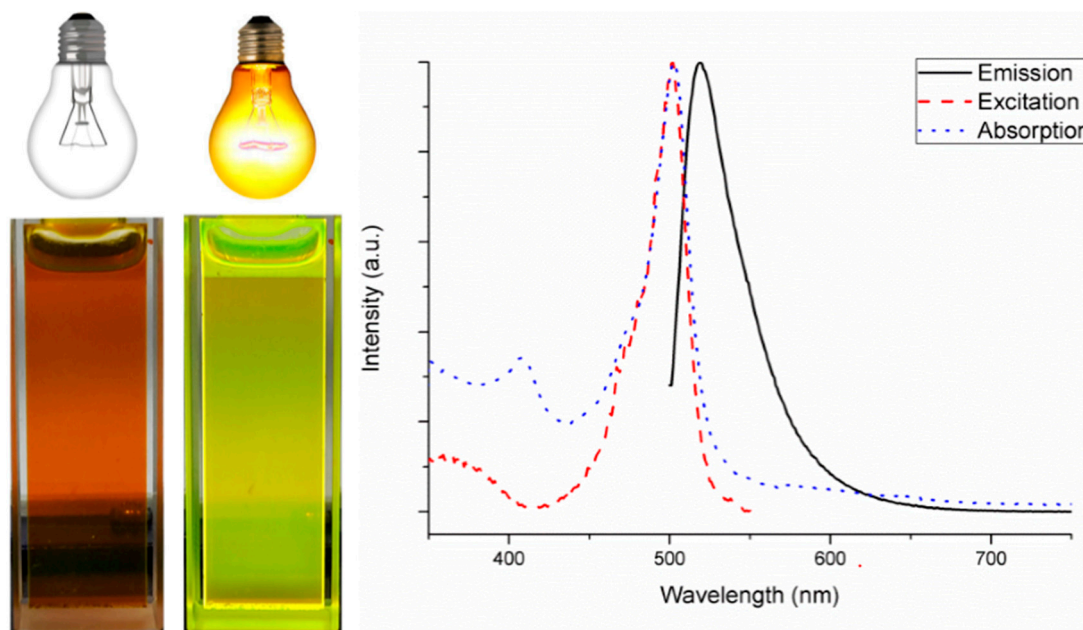

Figure 4. The emission (black line), excitation (red dashed line) and absorption (blue dotted line) spectrum of Gd-DOTA-BODIPY in water.

The fluorescent quantum yields Q_L of La-DOTA-BODIPY and Gd-DOTA-BODIPY were determined upon ligand excitation by a comparative method, using a solution of Rhodamine 6G ($Q = 78\%$) [67] in water as the standard. The advantage of BODIPY dyes is that the quantum yields of their derivatives are generally high, even in water [39]. The quantum yield was determined according to the following equation:

$$Q_L = Q_S \times \frac{I_X}{I_S} \times \frac{A_S(\lambda_{exc})}{A_X(\lambda_{exc})} \times \frac{\eta_X^2}{\eta_S^2} \qquad (1)$$

In this equation the s and x refer to the standard and the unknown sample respectively, I represents the corrected total integrated emission intensity, A: the absorbance at the excitation wavelength, η: the refractive index of the solution ($\eta_{water} = 1.33$), and Q_s: the quantum yield of the standard ($Q = 78\%$) [67]. The samples are diluted until the absorbance at the excitation wavelength is between 0.02–0.05. Quantum yield is recorded with ligand excitation wavelength of 490 nm and gave values of 80% and 83% for La-DOTA-BODIPY and Gd-DOTA-BODIPY, respectively.

2.3. Relaxivity of Gd-DOTA-BODIPY

The relaxivity r_1 is the efficiency of a 1 mM solution of gadolinium(III) agent to shorten the longitudinal relaxation time (T_1). According to the Solomon Bloembergen Morgan theory [68,69] several parameters can alter the relaxivity of a contrast agent. High relaxivity can be obtained with a higher amount of water molecules directly bound to the paramagnetic centre (q). Although an easy parameter to adjust, increasing the q value leads to less stable complexes. Other parameters are the distance between gadolinium(III) and water (r), the water residence time (τ_M), the rotational correlation time of the paramagnetic center (τ_R), the electronic relaxation time of gadolinium(III) at zero field (τ_{S0}) and the correlation time modulating the electronic relaxation (τ_v). The relaxivity of Gd-DOTA-BODIPY derivative measured at frequencies of 20 and 60 MHz at 310 K and was found to be 3.9 and 3.6 $s^{-1} \cdot mM^{-1}$ respectively. These values are in close comparison with previously reported values for Gd(III)-DOTA complex, which gave values of 3.5 and 3.1 $s^{-1} \cdot mM^{-1}$ at 20 and 60 MHz respectively [70]. A slight increase compared to the parent Gd-DOTA complex can be attributed to the increase in molecular weight of the Gd-DOTA-BODIPY complex, resulting in the increase of the rotational correlation time (τ_R) and in overall increase of the relaxivity. The limiting factors for the increase of Gd-DOTA-BODIPY relaxivity are probably the presence of an amide bond in the DOTA scaffold which may slow down the water exchange rate, or flexible linker used for attaching the BODIPY core to DOTA, which may result in high internal rotations within the Gd-DOTA-BODIPY.

3. Experimental Section

3.1. Materials, Reagents, and Solvents

β-alanine, boron trifluoride diethyl etherate, phosphoryl chloride, thionyl chloride was obtained from Sigma-Aldrich (Bornem, Belgium); Copper(II)sulphate, 2,4-dimethylpyrrole, dry dichloromethane, lanthanum(III) chloride heptahydrate, methanol, sodium ascorbate, triethylamine were purchased from Acros Organics (Geel, Belgium); acetonitrile, diethyl ether, ethyl acetate, petroleum ether, magnesium

sulphate from VWR chemicals (Leuven, Belgium); dichloromethane, from hydrogen chloride Fisher Scientific (Loughborough, UK); Gadolinium(III) was obtained from Alfa Aesar (Ward Hill, Shrewsbury, MA, USA) and were used without further purification.

3.2. Characterization

NMR spectra were measured on a Bruker Avance 300 (Bruker, Karlsruhe, Germany) (operating at 300 MHz for ^{1}H NMR spectra, operating at 75 MHz for ^{13}C NMR), Bruker Avance 400 (operating at 400 MHz for ^{1}H NMR spectra, operating at 100 MHz for ^{13}C NMR spectra). Chemical shifts are reported in parts per million (ppm) and are referenced to the internal standard tetramethylsilane. For ^{13}C spectra, residual solvent signals are used as the internal standard. Spectra are taken at room temperature unless otherwise stated. Relaxation rates at 20 and 60 MHz were obtained on a Minispec mq-20, and a Minispec mq-60 (Bruker, Karlsruhe, Germany) respectively.

FT-IR spectra were measured by using a Bruker Vertex 70 FT-IR spectrometer (Bruker, Ettlingen, Germany). ESI-MS measurements were taken on a Thermo Electron LCQ Advantage apparatus (Thermo Scientific, Waltham, MA, USA) with Agilent 1100 pump (Agilent, Waldbronn, Germany) and injection system coupled to Xcalibur data analyzing software. Methanol is used as eluent. TXRF measurements were done on a Bruker S2 Picofox (Bruker, Berlin, Germany) by analyzing approximately 100 ppm gadolinium or europium solutions with respect to a Chem-Lab gallium standard solution (500 µg/mL, 2%–5% HNO₃).

The flow setup was constructed with copper GC tubing (0.065″ inner diameter, Restek, Middelburg, Netherlands) and the reagents are pumped using a Chemyx Fusion 200 syringe pump (Chemyx, Stafford, TX, USA). LC–MS was performed on an Alltech Prevail RP-C18 5 µm 150 mm × 2.1 mm column coupled to an Agilent 1100 degasser, quaternary pump, auto sampler, UV-DAD detector, and thermostated column module coupled to Agilent 6110 single-quadrupole MS. Use of Agilent LC/MSD Chemstation software. HPLC was performed on Waters Delta 600 analytical/preparative system equipped with a Waters 996 Photo Diode Array detector (Waters, Milford, MA, USA). Preparative column: Alltech C18 Prevail 5 µm 150 mm × 22 mm.

UV-VIS absorption spectra were measured on a Varian Cary 5000 spectrophotometer (Agilent, Santa Clara, CA, USA) on freshly prepared aqua solutions in quartz Suprasil® cells (115F-QS) with an optical path-length of 1.0 cm. Excitation and emission data were recorded on an Edinburgh Instruments FS900 steady state spectrofluorimeter (Edinburgh Instruments, Livingston, UK). This instrument is equipped with a 450 W xenon arc lamp and an extended red-sensitive photomultiplier (Hamamatsu R 2658P). Quantum yields were determined by a comparative method with an estimated experimental error of ± 10% using a solution of Rhodamine 6G in water ($Q = 78\%$) as standard. The solutions are diluted to get an optical density lower than 0.05 at the excitation wavelength.

3.3. Synthetic Procedures

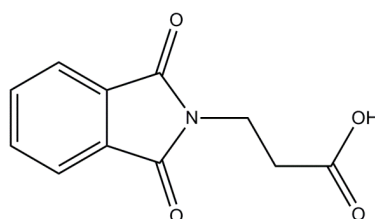3.3.1. Synthesis of Product (**1**) (Figure 5)

Figure 5. Chemical structure of Product **1**.

Phthalic anhydride (1 eq, 40 mmol, 5.92 g) and β-alanine (1 eq, 40 mmol, 3.56 g) were added in a round bottom flask and heated up to 160 °C for 6 h where it became a smelt. The mixture was cooled and the resulting solid was dissolved in DCM. The solution was washed with 0.1 M HCl (3 × 30 mL). The organic layer was dried with MgSO$_4$ and evaporated till dryness, yield: 5.68 g, 25.9 mmol, 65%. CI–MS (MeOH, *m/z*): calcd: 219.19 g/mol, found: 220.0 g/mol [M + H]$^+$. ^{1}H NMR (300 MHz, CDCl$_3$, δ ppm): 2.80 (t, *J* = 7.4 Hz, 2H), 4.00 (t, *J* = 7.4 Hz, 2H), 7.74 (m, 2H), 7.84 (m, 2H); ^{13}C NMR (75 MHz, CDCl$_3$, δ ppm): 32.8, 33.4, 123.4, 132.0, 134.1, 168.0, 176.5.

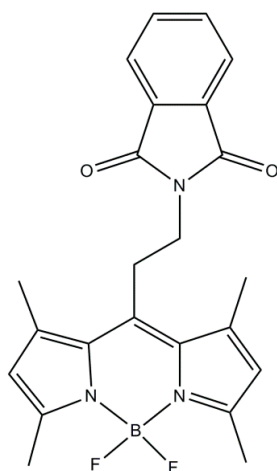3.3.2. Synthesis of BODIPY-(CH$_2$)$_2$-Phtalimide (**2**) (Figure 6)

Figure 6. Chemical structure of Product **2**.

To a round bottom flask product **1** (1 eq, 5 mmol, 1.10 g) and thionyl chloride (5 eq, 25 mmol, 1.82 mL) were added and refluxed for 3 h. The thionyl chloride was removed *in vacuo* until dryness. The acid chloride was used further without any purification. The yellow residue was dissolved in 30 mL dry DCM and 2,4-dimethylpyrrole (2 eq, 10 mmol, 1.04 mL) was slowly added. The solution was stirred for 30 min at room temperature. The color changed from yellow to red-brown. The solution was subsequently refluxed for 4 h. The solution was then cooled to 0 °C and triethylamine (10 eq, 50 mmol, 6.97 mL) was added. After 5 min of stirring at 0 °C boron trifluoride diethyl etherate (11 eq, 55 mmol, 6.79 mL) was slowly added and the solution was stirred overnight at room temperature. Diethyl ether (100 mL) was added to the solution and the organic layer was washed with water

(3 × 50 mL). The organic layer was dried with MgSO₄ and concentrated *in vacuo*. The resulting residue was purified using silica column (eluent: DCM/PET 50:50) yielding a dark orange solid, yield: 0.392 g, 0.9 mmol, 19%. CI–MS (MeOH, *m/z*): calcd: 421.25 g/mol, found: 421 g/mol [M]⁺. ¹H NMR (300 MHz, CDCl₃, δ ppm): 2.54 (s, 6H), 2.67 (s, 6H), 3.42 (t, *J* = 8.60 Hz, 2H), 3.89 (t, *J* = 8.60 Hz, 2H), 6.11 (s, 2H), 7.77 (m, 2H), 7.88 (m, 2H); ¹³C NMR (100 MHz, CDCl₃, δ ppm): 14.6, 16.4, 27.7, 39.0, 122.2, 123.5, 131.7, 131.9, 134.3, 139.8, 141.5, 154.9, 168.2.

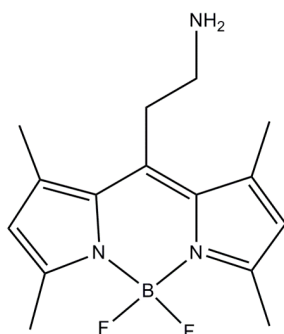### 3.3.3. Synthesis of BODIPY-(CH₂)₂-Amine (**3**) (Figure 7)

Figure 7. Chemical structure of Product **3**.

BODIPY-(CH₂)₂-phtalimide (**2**) (1 eq, 0.37 mmol, 158 mg) and hydrazine hydrate (1 eq, 0.37 mmol, 18.8 mg) in 20 mL ethanol was refluxed for 3 h. After which the solution was cooled to room temperature and filtrated with a Millipore 0.45 μM filter and the solvent was concentrated *in vacuo* until an orange solid, yield: 0.106, 0.36 mmol, 97%. CI–MS (MeOH, *m/z*): calcd: 291.17 g/mol, found: 282 g/mol [M − F]⁺, and 291 [M]⁺. ¹H NMR (300 MHz, CDCl₃, δ ppm): 1.61, (broad, 2H), 2.45 (s, 6H), 2.51 (s, 6H), 2.99 (m, 2H), 3.14 (m, 2H), 6.05 (s, 2H); ¹³C NMR (100 MHz, CDCl₃, δ ppm): 10.5, 12.6, 28.2, 40.1, 117.9, 127.8, 136.6, 138.9, 150.2.

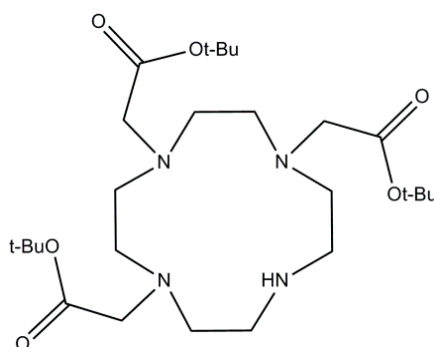### 3.3.4. Synthesis of DO3A-tBu (**4**) (Figure 8)

Figure 8. Chemical structure of Product **4**.

The synthesis uses an altered synthesis by Viguier *et al.* [58]. To a solution of tetraazacyclodedecaan (1 eq, 5.80 mmol, 1 g), sodium bicarbonate (3.5 eq, 20.3 mmol, 1.71 g) in 150 mL ACN under an argon atmosphere a solution of tert-butyl bromoacetate (3.5 eq, 20.3 mmol, 3.0 mL) in 50 mL ACN was added drop wise. The mixture was refluxed for 17 h. After removing the

salts via filtration over Celite® the solvent was evaporated and the solid was recrystallized from toluene as a white powder, yield: 2.47 g, 4.8 mmol, 82%. ESI–MS: *m/z* calcd 516 [M + H]+, 538 [M + Na]+, found 516.0 [M + H]+, 537.5 [M + Na]+. ^{1}H NMR (CDCl₃, 300 MHz, δ ppm): 1.46 (s, 27H), 2.88 (t, 12H), 3.08 (t, 4H), 3.30 (s, 2H), 3.38 (s, 4H). ^{13}C NMR (CDCl₃, 75 MHz, δ ppm): 28.2, 28.3, 47.5, 49.5, 51.3, 58.1, 81.6, 81.7, 169.8, 170.6.

3.3.5. Synthesis of {4,10-Bis-Tert-Butoxycarbonylmethyl-7-[(2-Propynylcarbamoyl)-Methyl]-1,4,7,10-Tetraaza-Cyclododec-1-yl}-Acetic Acid Tert-Butyl Ester (**5**) (Figure 9)
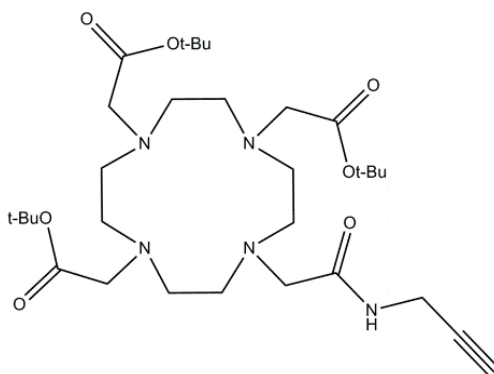

Figure 9. Chemical structure of Product **5**.

A solution of DO3A-tBu (**4**) (1 eq, 772 mg, 1.5 mmol), *N*-(2-propynyl)chloroacetamide (1.2 eq, 291 mg, 1.8 mmol) and K₂CO₃ (2 eq, 415 mg, 3.0 mmol) in 70 mL ACN was stirred under nitrogen at reflux temperature for 17 h. After filtration of over Celite®, the solvent was removed *in vacuo*, the residual mixture was purified by basic alumina (eluens CHCl₃:MeOH (98:2)) to give a colorless solid, yield: 1.45 g, 2.4 mmol, 94%. ESI–MS: *m/z* calcd 610.80 [M + H]+, found 632 [M + Na]+. ^{1}H NMR (CDCl₃, 300 MHz, δ ppm): 1.45 (s, 18H), 1.46 (s, 9H), 2.15 (t, *J* = 2.3 Hz, 1H), 2.52 (broad, 4H), 2.70 (broad, 4H), 2.82 (broad, 4H), 2.91 (broad, 4H), 3.10 (s, 2H), 3.27 (s, 4H), 3.38 (s, 2H), 4.05 (dd, *J* = 5.5 Hz, *J* = 2.3 Hz, 2H), 9.27 (t, *J* = 5.5 Hz, 1H). ^{13}C NMR (CDCl₃, 75 MHz, δ ppm): 28.2, 28.3, 28.6, 29.3, 52.1, 52.5, 53.8, 55.2, 56.2, 57.6, 70.2, 72.9, 80.9, 170.8.

3.3.6. Synthesis of {4,10-Bis-Carboxymethyl-7-[(2-Propynylcarbamoyl)-Methyl]-1,4,7,10-Tetraaza-Cyclododec-1-yl}-Acetic Acid (**6**) (Figure 10)
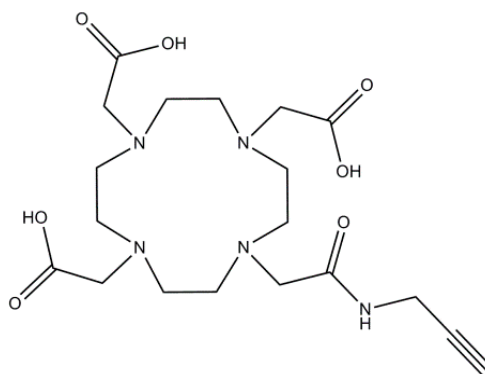

Figure 10. Chemical structure of Product **6**.

Product (**5**) (1 eq, 1.45 g, 2.4 mmol) was dissolved in 10 mL of a DCM/TFA (50:50) mixture and stirred under inert atmosphere overnight. After the reaction, 20 mL of DCM was added and evaporated (repeated two times), yield: 1.07 g, 2.4 mmol, quantitative. ESI-MS: *m/z* calcd 442.22 $[M + H]^+$, found 442 $[M + H]^+$, 464 $[M + Na]^+$. ^{1}H NMR (D$_2$O, 300 MHz, δ ppm): 2.42 (t, 1H), 2.48–4.01 (broad, 22H), 3.81 (broad, 2H). ^{13}C NMR (D$_2$O, 75 MHz, δ ppm): 29.1, 29.6, 49.7, 53.7, 58.6, 60.6, 60.8, 69.3, 72.7, 73.5, 78.7, 175.4, 179.4, 179.6.

3.3.7. Synthesis of Lanthanide(III) {4,10-Bis-Carboxymethyl-7-[(2-Propynylcarbamoyl)-Methyl]-1,4,7,10-Tetraaza-Cyclododec-1-yl}-Acetic Acid (Figure 11)
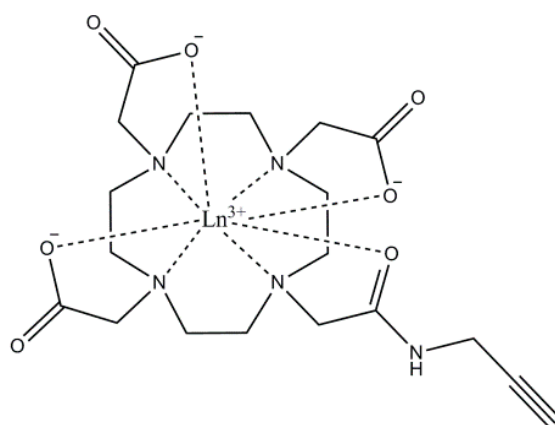

Figure 11. Chemical structure of Products **7** and **8**.

General procedure for complexation of propargylated DOTA: Product (**6**) (1 eq) was dissolved in 5 mL water and the appropriate lanthanide(III) chloride hydrate (1,1 eq) was added. The pH was adjusted to 5.5 with a 0.1 M KOH solution and stirred overnight at 60 °C. The solvent was evaporated. The residue was redissolved in 5 mL water and Chelex-100 was added and stirred for 2 h. This last step was repeated until no free lanthanide was found with an Arsenazo III indicator [71].

Propargylated Gd-DOTA (**7**): Yield: 0.446 g, 0.75 mmol, 67%. ESI-MS: *m/z* calcd 596.70 $[M + H]^+$, found 619.2 $[M + Na]^+$. IR (neat): 3416, 3245, 3098, 2873, 1675, 1609 cm^{-1}.

Propargylated La-DOTA (**8**): Yield: 0.445 g, 0.77 mmol, 65%. ESI-MS: *m/z* calcd 478.36 $[M + H]^+$, found 600.5 $[M + Na]^+$. ^{1}H NMR (CDCl$_3$, 300 MHz, δ ppm): 2.42 (t, 1H), 2.48–4.01 (broad, 22H), 3.81 (broad, 2H). ^{13}C NMR (CDCl$_3$, 75 MHz, δ ppm): 29.1, 29.6, 49.7, 53.7, 58.5, 60.6, 60.8, 69.2, 72.7, 73.5, 78.7, 175.4, 179.4, 179.6; IR (neat): 3429, 3258, 3103, 2857, 1673, 1606 cm^{-1}.

3.3.8. General Procedure Flow

Stock solution A: a 2 mL solution in a degassed mixture of 10:3:3 MeOH:DCM:H$_2$O of 1 eq BODIPY-amine and 11 equivalents of DIPEA.

Stock solution B: a 2 mL solution of three equivalents of ISA·H$_2$SO$_4$ in a degassed mixture of 10:3:3 MeOH:DCM:H$_2$O.

Both solutions in a separate syringe are combined via a T-mixer in an ice bath before introducing the mixture to the copper tube flow reactor (150 μL) at room temperature. Flow speed is adjusted so the retention time in the reactor is 300 s. The column is stabilized during three reactor volumes. Upon

leaving the reactor, the reaction mixture was directly added to a solution of 1.5 equivalent of Ln-DOTA-propargyl and 1.5 eq sodium ascorbate. The mixture is left stirring overnight. The aqueous layer is lyophilized, redissolved in distilled water, purified via HPLC and lyophilized. The products are isolated as bright orange powders.

Product **9** (Gd) (Figure 12): Yield: 13 mg, 0.01 mmol, 6%. ESI–MS: *m/z* calcd 913.85 [M + H]$^+$, found 913.2 [M + H]$^+$. The concentration used for relaxivity was 1.45 mmol/L and was measured by TXRF against an internal gallium standard.

Product **10** (La) (Figure 12): Yield: 23 mg, 0.03 mmol, 9%. ESI-MS: *m/z* calcd 895.51 [M + H]$^+$, found 917.8 [M + Na]$^+$ (positive mode), 894.2 [M + e]$^-$ (negative mode). ^{1}H NMR (D$_2$O, 300 MHz, δ ppm): 2.08 (s, 6H), 2.20 (s, 6H), 2.20–3.82 (broad, 26H), 4.33 (broad, H), 6.00 (s, 2H), 7.55 (s, 1H). ^{11}B NMR (D$_2$O, 80 MHz, δ ppm): 2.16 ppm with respect to B(OMe)$_3$ as a reference.
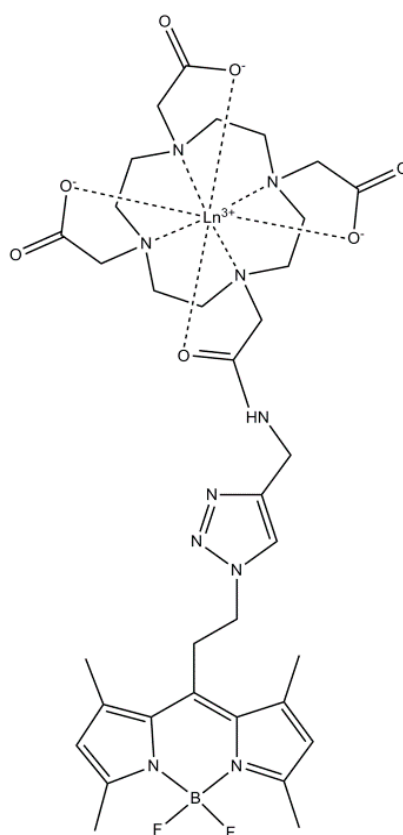

Figure 12. Chemical structure of Products **9** and **10**.

After each reaction the copper tube flow reactor is cleansed in a sonication bath for 10 min while introducing a 1:1 mixture of MeOH:triethylamine at 4 mL/min, followed by 20 mL of pentane at 4 mL/min. The reactor is dried with argon and stored under argon.

4. Conclusions

In this paper a novel Gd-DOTA-BODIPY derivative is synthesized via a diazotransfer reaction under flow conditions in a copper tube. The complex is water-soluble and exhibits favorable fluorescent properties, thus offering the possibility for the use of BODIPY adducts for *in vivo* optical imaging. High quantum yield of 83% is obtained in water, and bright emission was observed at

523 nm. Shifting of the emission to the more optimal red-IR region of the spectrum will be attempted in future by increasing the electronic resonance of the BODIPY by adding appropriate substituents to the BODIPY core. The complex exhibits relaxivities which are comparable to the parent Gd-DOTA complex and, therefore, holds potential as a bimodal contrast agent for MRI and optical imaging.

Supplementary Materials

Supplementary materials can be found at http://www.mdpi.com/2304-6740/3/4/0516/s1.

Acknowledgments

Author Contributions

Matthias Ceulemans and Koen Nuyts have performed experimental work and spectroscopic measurements. Wim M. De Borggraeve and Tatjana N. Parac-Vogt have supervised the work and helped with interpretation of the results sand the writing of the final manuscript.

Conflicts of Interest

The authors declare no conflict of interest.

References

1. Hermann, P.; Kotek, J.; Kubícek, V.; Lukes, I. Gadolinium(III) complexes as MRI contrast agents: Ligand design and properties of the complexes. *Dalton Trans.* **2008**, *9226*, 3027–3047.
2. Pierre, V.C.; Allen, M.J.; Caravan, P. Contrast agents for MRI: 30+ years and where are we going? *J. Biol. Inorg. Chem.* **2014**, *19*, 127–131.
3. Waters, E.A.; Wickline, S.A. Contrast agents for MRI. *Basic Res. Cardiol.* **2008**, *103*, 114–121.
4. Tóth, É.; Helm, L.; Merbach, A. Contrast Agents I. In *Topics in Current Chemistry*; Krause, W., Ed.; Springer Berlin Heidelberg: Berlin, Germany, 2002; Volume 221, pp. 61–101.
5. Debroye, E.; Parac-Vogt, T.N. Towards polymetallic lanthanide complexes as dual contrast agents for magnetic resonance and optical imaging. *Chem. Soc. Rev.* **2014**, *43*, 8178–8192.
6. Cacheris, W.P.; Quay, S.C.; Rocklage, S.M. The relationship between thermodynamics and the toxicity of gadolinium complexes. *Magn. Reson. Imaging* **1990**, *8*, 467–481.
7. Shellock, F.G.; Kanal, E. Safety of magnetic resonance imaging contrast agents. *J. Magn. Reson. Imaging* **1999**, *10*, 477–484.
8. Bartolini, M.E.; Pekar, J.; Chettle, D.R.; McNeill, F.; Scott, A.; Sykes, J.; Prato, F.S.; Moran, G.R. An investigation of the toxicity of gadolinium based MRI contrast agents using neutron activation analysis. *Magn. Reson. Imaging* **2003**, *21*, 541–544.
9. Accardo, A.; Tesauro, D.; Aloj, L.; Pedone, C.; Morelli, G. Supramolecular aggregates containing lipophilic Gd(III) complexes as contrast agents in MRI. *Coord. Chem. Rev.* **2009**, *253*, 2193–2213.

10. Caravan, P.; Ellison, J.J.; McMurry, T.J.; Lauffer, R.B. Gadolinium(III) chelates as MRI contrast agents: Structure, dynamics, and applications. *Chem. Rev.* **1999**, *99*, 2293–2352.

11. Villaraza, A.J.L.; Bumb, A.; Brechbiel, M.W. Macromolecules, dendrimers, and nanomaterials in magnetic resonance imaging: The interplay between size, function, and pharmacokinetics. *Chem. Rev.* **2010**, *110*, 2921–2959.

12. Sherry, A.D.; Brown, R.D.; Geraldes, C.F.G.C.; Koenig, S.H.; Kuan, K.-T.; Spiller, M. Synthesis and characterization of the gadolinium(3+) complex of DOTA-propylamide: A model DOTA-protein conjugate. *Inorg. Chem.* **1989**, *28*, 620–622.

13. Huang, W.-Y.; Davis, J.J. Multimodality and nanoparticles in medical imaging. *Dalton Trans.* **2011**, *40*, 6087–6103.

14. Xie, J.; Liu, G.; Eden, H.S.; Ai, H.; Chen, X. Surface-engineered magnetic nanoparticle platforms for cancer imaging and therapy. *Acc. Chem. Res.* **2011**, *44*, 883–892.

15. Louie, A. Multimodality imaging probes: Design and challenges. *Chem. Rev.* **2010**, *110*, 3146–3195.

16. Joshi, B.P.; Wang, T.D. Exogenous molecular probes for targeted imaging in cancer: Focus on multi-modal imaging. *Cancers (Basel)* **2010**, *2*, 1251–1287.

17. Soenen, S.J.; Vande Velde, G.; Ketkar-Atre, A.; Himmelreich, U.; de Cuyper, M. Magnetoliposomes as magnetic resonance imaging contrast agents. *Wiley Interdiscip. Rev. Nanomed. Nanobiotechnol.* **2002**, *3*, 197–211.

18. Costa, J.; Ruloff, R.; Burai, L.; Helm, L.; Merbach, A.E. Rigid M(II)L$_2$Gd$_2$(III) (M = Fe, Ru) complexes of a terpyridine-based heteroditopic chelate: A class of candidates for MRI contrast agents. *J. Am. Chem. Soc.* **2005**, *127*, 5147–5157.

19. Livramento, J.B.; Sour, A.; Borel, A.; Merbach, A.E.; Tóth, É. A starburst-shaped heterometallic compound incorporating six densely packed Gd^{3+} Ions. *Chem. Eur. J.* **2006**, *12*, 989–1003.

20. Livramento, J.B.; Weidensteiner, C.; Prata, M.I.M.; Allegrini, P.R.; Geraldes, C.F.G.C.; Helm, L.; Kneuer, R.; Merbach, A.E.; Santos, A.C.; Schmidt, P.; *et al.* First *in vivo* MRI assessment of a self-assembled metallostar compound endowed with a remarkable high field relaxivity. *Contrast Media Mol. Imaging* **2006**, *1*, 30–39.

21. Parac-Vogt, T.N.; Vander Elst, L.; Kimpe, K.; Laurent, S.; Burtéa, C.; Chen, F.; van Deun, R.; Ni, Y.; Muller, R.N.; Binnemans, K. Pharmacokinetic and *in vivo* evaluation of a self-assembled gadolinium(III)-iron(II) contrast agent with high relaxivity. *Contrast Media Mol. Imaging* **2006**, *1*, 267–278.

22. Paris, J.; Gameiro, C.; Humblet, V.; Mohapatra, P.K.; Jacques, V.; Desreux, J.F. Auto-assembling of ditopic macrocyclic lanthanide chelates with transition-metal ions. Rigid multimetallic high relaxivity contrast agents for magnetic resonance imaging. *Inorg. Chem.* **2006**, *45*, 5092–5102.

23. Dehaen, G.; Verwilst, P.; Eliseeva, S.V.; Laurent, S.; Vander Elst, L.; Muller, R.N.; de Borggraeve, W.M.; Binnemans, K.; Parac-Vogt, T.N. A heterobimetallic ruthenium-gadolinium complex as a potential agent for bimodal imaging. *Inorg. Chem.* **2011**, *50*, 10005–10014.

24. Dehaen, G.; Eliseeva, S.V.; Kimpe, K.; Laurent, S.; Vander Elst, L.; Muller, R.N.; Dehaen, W.; Binnemans, K.; Parac-Vogt, T.N.; Vanderelst, L.; *et al.* A self-assembled complex with a titanium(IV) catecholate core as a potential bimodal contrast agent. *Chem. Eur. J.* **2012**, *18*, 293–302.

25. Verwilst, P.; Eliseeva, S.V.; Vander Elst, L.; Burtea, C.; Laurent, S.; Petoud, S.; Muller, R.N.; Parac-Vogt, T.N.; de Borggraeve, W.M. A tripodal ruthenium-gadolinium metallostar as a potential $\alpha_v\beta_3$ integrin specific bimodal imaging contrast agent. *Inorg. Chem.* **2012**, *51*, 6405–6411.

26. Dehaen, G.; Eliseeva, S.V.; Verwilst, P.; Laurent, S.; Vander Elst, L.; Muller, R.N.; de Borggraeve, W.M.; Binnemans, K.; Parac-Vogt, T.N. Tetranuclear d-f metallostars: Synthesis, relaxometric, and luminescent properties. *Inorg. Chem.* **2012**, *51*, 8775–8783.

27. Debroye, E.; Ceulemans, M.; Vander Elst, L.; Laurent, S.; Muller, R.N.; Parac-Vogt, T.N. Controlled synthesis of a novel heteropolymetallic complex with selectively incorporated lanthanide(III) ions. *Inorg. Chem.* **2014**, *53*, 1257–1259.

28. Kuil, J.; Buckle, T.; Oldenburg, J.; Yuan, H.; Borowsky, A.D.; Josephson, L.; van Leeuwen, F.W.B. Hybrid peptide dendrimers for imaging of chemokine receptor 4 (CXCR4) expression. *Mol. Pharm.* **2011**, *8*, 2444–2453.

29. Musonda, C.C.; Taylor, D.; Lehman, J.; Gut, J.; Rosenthal, P.J.; Chibale, K. Application of multi-component reactions to antimalarial drug discovery. Part 1: Parallel synthesis and antiplasmodial activity of new 4-aminoquinoline Ugi adducts. *Bioorganic Med. Chem. Lett.* **2004**, *14*, 3901–3905.

30. Rivas, C.; Stasiuk, G.J.; Sae-Heng, M.; Long, N.J. Towards understanding the design of dual-modal MR/fluorescent probes to sense zinc ions. *Dalton Trans.* **2015**, *44*, 4976–4985.

31. Hüber, M.M.; Staubli, A.B.; Kustedjo, K.; Gray, M.H.B.; Shih, J.; Fraser, S.E.; Jacobs, R.E.; Meade, T.J. Fluorescently detectable magnetic resonance imaging agents. *Bioconjug. Chem.* **1998**, *9*, 242–249.

32. Mishra, A.A.K.; Pfeuffer, J.; Mishra, R.; Engelmann, J.; Mishra, A.A.K.; Ugurbil, K.; Logothetis, N.K. A new class of Gd-based DO3A-ethylamine-derived targeted contrast agents for MR and optical imaging. *Bioconjug. Chem.* **2006**, *17*, 773–780.

33. Zhang, M.; Imm, S.; Bähn, S.; Neubert, L.; Neumann, H.; Beller, M. Efficient copper(II)-catalyzed transamidation of non-activated primary carboxamides and ureas with amines. *Angew. Chem. Int. Ed.* **2012**, *51*, 3905–3909.

34. Jang, J.H.; Bhuniya, S.; Kang, J.; Yeom, A.; Hong, K.S.; Kim, J.S. Cu^{2+}-responsive bimodal (optical/MRI) contrast agent for cellular imaging. *Org. Lett.* **2013**, *15*, 4702–4705.

35. Ulrich, G.; Ziessel, R.; Harriman, A. The chemistry of fluorescent bodipy dyes: Versatility unsurpassed. *Angew. Chem. Int. Ed.* **2008**, *47*, 1184–1201.

36. Yee, M.-C.; Fas, S.C.; Stohlmeyer, M.M.; Wandless, T.J.; Cimprich, K.A. A cell-permeable, activity-based probe for protein and lipid kinases. *J. Biol. Chem.* **2005**, *280*, 29053–29059.

37. West, R.; Panagabko, C.; Atkinson, J. Synthesis and characterization of BODIPY-α-tocopherol: A fluorescent form of vitamin E. *J. Org. Chem.* **2010**, *75*, 2883–2892.

38. Kowada, T.; Maeda, H.; Kikuchi, K. BODIPY-based probes for the fluorescence imaging of biomolecules in living cells. *Chem. Soc. Rev.* **2015**, *44*, 4953–4972.

39. Boens, N.; Leen, V.; Dehaen, W. Fluorescent indicators based on BODIPY. *Chem. Soc. Rev.* **2012**, *41*, 1130–1172.

40. García-Moreno, I.; Amat-Guerri, F.; Liras, M.; Costela, A.; Infantes, L.; Sastre, R.; López Arbeloa, F.; Bañuelos Prieto, J.; López Arbeloa, Í. Structural changes in the BODIPY dye PM567 enhancing the laser action in liquid and solid media. *Adv. Funct. Mater.* **2007**, *17*, 3088–3098.

41. Duran-Sampedro, G.; Agarrabeitia, A.R.; Garcia-Moreno, I.; Costela, A.; Bañuelos, J.; Arbeloa, T.; López Arbeloa, I.; Chiara, J.L.; Ortiz, M.J. Chlorinated BODIPYs: Surprisingly efficient and highly photostable laser dyes. *Eur. J. Org. Chem.* **2012**, *2012*, 6335–6350.

42. Lakshmi, V.; Rajeswara Rao, M.; Ravikanth, M. Halogenated boron-dipyrromethenes: Synthesis, properties and applications. *Org. Biomol. Chem.* **2015**, *13*, 2501–2517.

43. Bessette, A.; Hanan, G.S. Design, synthesis and photophysical studies of dipyrromethene-based materials: Insights into their applications in organic photovoltaic devices. *Chem. Soc. Rev.* **2014**, *43*, 3342.

44. Singh, S.P.; Gayathri, T. Evolution of BODIPY dyes as potential sensitizers for dye-sensitized solar cells. *Eur. J. Org. Chem.* **2014**, *2014*, 4689–4707.

45. González-Béjar, M.; Liras, M.; Francés-Soriano, L.; Voliani, V.; Herranz-Pérez, V.; Duran-Moreno, M.; Garcia-Verdugo, J.M.; Alarcon, E.I.; Scaiano, J.C.; Pérez-Prieto, J. NIR excitation of upconversion nanohybrids containing a surface grafted bodipy induces oxygen-mediated cancer cell death. *J. Mater. Chem. B* **2014**, *2*, 4554.

46. Lim, S.H.; Thivierge, C.; Nowak-Sliwinska, P.; Han, J.; van den Bergh, H.; Wagnières, G.; Burgess, K.; Lee, H.B. *In vitro* and *in vivo* photocytotoxicity of boron dipyrromethene derivatives for photodynamic therapy. *J. Med. Chem.* **2010**, *53*, 2865–2874.

47. Bernhard, C.; Goze, C.; Rousselin, Y.; Denat, F. First bodipy–DOTA derivatives as probes for bimodal imaging. *Chem. Commun.* **2010**, *46*, 8267.

48. Bernhard, C.; Moreau, M.; Lhenry, D.; Goze, C.; Boschetti, F.; Rousselin, Y.; Brunotte, F.; Denat, F. DOTAGA-anhydride: A valuable building block for the preparation of DOTA-like chelating agents. *Chem. Eur. J.* **2012**, *18*, 7834–7841.

49. Iwaki, S.; Hokamura, K.; Ogawa, M.; Takehara, Y.; Muramatsu, Y.; Yamane, T.; Hirabayashi, K.; Morimoto, Y.; Hagisawa, K.; Nakahara, K.; *et al*. A design strategy for small molecule-based targeted MRI contrast agents: Their application for detection of atherosclerotic plaques. *Org. Biomol. Chem.* **2014**, *12*, 8611–8618.

50. Yamane, T.; Hanaoka, K.; Muramatsu, Y.; Tamura, K.; Adachi, Y.; Miyashita, Y.; Hirata, Y.; Nagano, T. Method for enhancing cell penetration of Gd^{3+}-based MRI contrast agents by conjugation with hydrophobic fluorescent dyes. *Bioconjug. Chem.* **2011**, *22*, 2227–2236.

51. Duheron, V.; Moreau, M.; Collin, B.; Sali, W.; Bernhard, C.; Goze, C.; Gautier, T.; Pais de Barros, J.-P.; Deckert, V.; Brunotte, F.; *et al*. Dual labeling of lipopolysaccharides for SPECT-CT imaging and fluorescence microscopy. *ACS Chem. Biol.* **2014**, *9*, 656–662.

52. Lhenry, D.; Larrouy, M.; Bernhard, C.; Goncalves, V.; Raguin, O.; Provent, P.; Moreau, M.; Collin, B.; Oudot, A.; Vrigneaud, J.-M.; *et al*. BODIPY: A highly versatile platform for the design of bimodal imaging probes. *Chemistry* **2015**, *21*, 13091–13099.

53. Hendricks, J.A.; Keliher, E.J.; Wan, D.; Hilderbrand, S.A.; Weissleder, R.; Mazitschek, R. Synthesis of [18F]BODIPY: Bifunctional reporter for hybrid optical/positron emission tomography imaging. *Angew. Chem. Int. Ed. Engl.* **2012**, *51*, 4603–4606.

54. Liu, S.; Li, D.; Zhang, Z.; Surya Prakash, G.K.; Conti, P.S.; Li, Z. Efficient synthesis of fluorescent-PET probes based on [18F]BODIPY dye. *Chem. Commun.* **2014**, *50*, 7371.

55. Nuyts, K.; Ceulemans, M.; Parac-Vogt, T.N.; Bultynck, G.; de Borggraeve, W.M. Facile azide formation via diazotransfer reaction in a copper tube flow reactor. *Tetrahedron Lett.* **2015**, *56*, 1687–1690.

56. Fischer, N.; Goddard-Borger, E.D.; Greiner, R.; Klapötke, T.M.; Skelton, B.W.; Stierstorfer, J. Sensitivities of some imidazole-1-sulfonyl azide salts. *J. Org. Chem.* **2012**, *77*, 1760–1764.

57. Hansen, A.M.; Sewell, A.L.; Pedersen, R.H.; Long, D.-L.; Gadegaard, N.; Marquez, R. Tunable BODIPY derivatives amenable to "click" and peptide chemistry. *Tetrahedron* **2013**, *69*, 8527–8533.

58. Viguier, R.F.H.; Hulme, A.N. A sensitized europium complex generated by micromolar concentrations of copper(I): Toward the detection of copper(I) in biology. *J. Am. Chem. Soc.* **2006**, *128*, 11370–11371.

59. Verwilst, P.; Eliseeva, S.V.; Carron, S.; Vander Elst, L.; Burtea, C.; Dehaen, G.; Laurent, S.; Binnemans, K.; Muller, R.N.; Parac-Vogt, T.N.; *et al*. A modular approach towards the synthesis of target-specific MRI contrast agents. *Eur. J. Inorg. Chem.* **2011**, *2011*, 3577–3585.

60. Hessel, V.; Kralisch, D.; Kockmann, N.; Noël, T.; Wang, Q. Novel process windows for enabling, accelerating, and uplifting flow chemistry. *ChemSusChem* **2013**, *6*, 746–789.

61. Johansson, H.; Pedersen, D.S. Azide- and alkyne-derivatised α-amino acids. *Eur. J. Org. Chem.* **2012**, *2012*, 4267–4281.

62. Goddard-Borger, E.D.; Stick, R.V. An efficient, inexpensive, and shelf-stable diazotransfer reagent: Imidazole-1-sulfonyl azide hydrochloride. *Org. Lett.* **2007**, *9*, 3797–3800.

63. Duimstra, J.A.; Femia, F.J.; Meade, T.J. A gadolinium chelate for detection of β-glucuronidase: A self-immolative approach. *J. Am. Chem. Soc.* **2005**, *127*, 12847–12855.

64. Wang, L.; Verbelen, B.; Tonnelé, C.; Beljonne, D.; Lazzaroni, R.; Leen, V.; Dehaen, W.; Boens, N. UV-VIS spectroscopy of the coupling products of the palladium-catalyzed C–H arylation of the BODIPY core. *Photochem. Photobiol. Sci.* **2013**, *12*, 835–847.

65. Kobayashi, H.; Ogawa, M.; Alford, R.; Choyke, P.L.; Urano, Y. New strategies for fluorescent probe design in medical diagnostic imaging. *Chem. Rev.* **2010**, *110*, 2620–2640.

66. Niu, S. Advanced Water Soluble BODIPY Dyes: Synthesis and Application. Ph.D. Thesis, Université de Strasbourg, Strasbourg, France, July 2011.

67. Olmsted, J. Calorimetric determinations of absolute fluorescence quantum yields. *J. Phys. Chem.* **1979**, *83*, 2581–2584.

68. Solomon, I. Relaxation processes in a system of two spins. *Phys. Rev.* **1955**, *99*, 559–565.

69. Bloembergen, N. Proton relaxation times in paramagnetic solutions. *J. Chem. Phys.* **1957**, *27*, 572.

70. Laurent, S.; Elst, L.V.; Muller, R.N. Comparative study of the physicochemical properties of six clinical low molecular weight gadolinium contrast agents. *Contrast Media Mol. Imaging* **2006**, *1*, 128–137.

71. Onishi, H. Spectrophotometric determination of zirconium, uranium, thorium and rare earths with arsenazo III after extractions with thenoyltrifluoroacetone and tri-*n*-octylamine. *Talanta* **1972**, *19*, 473–478.